Approach to wetting-layer-assisted lateral coupling of InAs/InP quantum dots

C. Cornet,* C. Platz, P. Caroff, J. Even, C. Labbé, H. Folliot, A. Le Corre, and S. Loualiche
LENS-UMR FOTON 6082 au CNRS, INSA de Rennes, 20 Avenue des Buttes de Coesmes, CS 14315, F34043 Rennes Cedex, France
(Received 31 January 2005; revised manuscript received 4 May 2005; published 20 July 2005)

We present new results on the simulation of two-dimensional (2D) quantum dot(s) (QDs) InAs/InP superlattices, emitting at 1.55 μm, the optical telecommunication wavelength. QDs and wetting layer (WL) electronic energy states are close in such a system. Using the Fourier-transformed Schrödinger equation developed on a mixed basis, we describe the wetting layer-assisted inter-QDs lateral (WLaiQD) coupling by studying the influence of WL states on QDs states and *vice versa*. The results show that WL and QDs have to be considered as a unique system, in strong coupling conditions. The increase of QDs density on the WL leads to enhanced splitting and miniband effects on QDs states. It induces a fragmentation of WL density of states interpreted as a 0D-like confinement of WL states. A comparison is made with a real high QDs density sample. It is expected to have an impact on carrier-capture phenomena in optoelectronic devices using high-density QDs in the active region.

DOI: 10.1103/PhysRevB.72.035342 PACS number(s): 73.21.La, 71.15.−m

I. INTRODUCTION

Recent research developments were devoted to nanostructured semiconductor materials. Quantum dots (QDs) may improve properties as compared to semiconductor quantum wells (QWs) for high-performance optoelectronic devices.[1–4] Most of the theoretically predicted QD properties have been experimentally demonstrated in the InAs/GaAs system.[5–7] In order to reach 1.55 μm wavelength used in optical telecommunications, QDs are usually grown on InP substrates.[8–10] Growth on (113)B substrate orientation leads to good quality QD structures with high densities and low size dispersion. The formation of a WL is a direct consequence of the Stransky-Krastanov growth mode. An original double cap method has been developed for controlling the QDs emission energy.[10] Optical characterizations of QDs ground state (GS), excited states (ES), and wetting layer states (WL) have been obtained by photoluminescence (PL),[10,11] Fourier transformed infrared (FTIR) spectroscopy,[11] and time-resolved photoluminescence (TRPL)[12,13] experiments. In Refs. 10 and 11, two PL emission lines are obtained at low temperature, interpreted as QDs optical ground state and WL ground state transitions. By considering WL and QDs as independent objects, we have succeeded in obtaining a first description of the electronic properties of these QDs using simple one-band effective mass models.[14] However, only one QD ground transition PL emission is obtained at room temperature. In Refs. 11–13, we observe an energy continuum between QD optical transitions and WL transitions. Moreover, TRPL and FTIR experimental observations may be interpreted by introducing a WL/QD coupling.[13] Kamerer *et al.*[15] have already pointed out the influence of the environment on the QDs properties and especially of the WL. Melnik *et al.* have shown that single QD electronic states are affected by the presence of the WL, based on one-band model equations.[16] Johnson *et al.*[17,18] studied a 30 QD lattice and found partial confinement in WL and partially delocalized heavy hole states in order to interpret the Robinson *et al.* measurements.[19–21] In theses calculations, periodic boundaries conditions are used to describe infinitely extended WL states. However, the influence of QD density (QDD) on QD electronic properties has not been studied in these references. For the first time, to our knowledge, the reciprocal space calculation[22,23] is applied as a new approach of the coupling problem in the (QD+WL) system. In the present work, we calculate in a very simple way the electronic structure of a 2D superlattice of cylindrical InAs/InP QDs on a WL. The main emphasis is given to the description of the WlaiQD coupling, and to the influence of QDD on coupling. A comparison with a real QD system is also made.

II. THEORY

Our goal is to describe the whole (QD+WL) system. Many conventional calculation methods, like finite differences, are based on a cell calculation.[16,19–21,24] The electronic wave functions usually vanish on the cell boundaries. These conditions do not allow us to describe delocalized wave functions for infinite objects like a WL. Therefore we choose a reciprocal description of our periodic system.[22,23] By developing wave functions on a k basis, we can easily describe continuum states, and the coupling between WL states and QD states. The Fourier-transformed (FT) Schrödinger equation is then solved for conduction band states:

$$\left\langle \vec{k}' \left| -\frac{\hbar^2}{2}\vec{\nabla}\frac{1}{m^*(\vec{r})}\vec{\nabla}\sum_{\vec{k}} c_{\vec{k}} \right| \vec{k} \right\rangle + \sum_{\vec{k}} c_{\vec{k}} \langle \vec{k}' | V(\vec{r}) | \vec{k} \rangle = E \left\langle \vec{k}' \left| \sum_{\vec{k}} c_{\vec{k}} \right| \vec{k} \right\rangle, \quad (1)$$

The confinement potential is equal to V_0=423 meV in all the confining volume, i.e., in all the InAs composed volume (QD and WL). Other parts of our structure (InP parts) have a V=0 potential.[25] We choose parabolic, anisotropic, and inhomogeneous effective masses[14] for the kinetic Hamiltonian part. The FT confinment potential $V_{\vec{k},\vec{k}'}=\langle \vec{k}' | V(\vec{r}) | \vec{k} \rangle$ is calculated analytically. The Hamiltonian diagonalization is per-

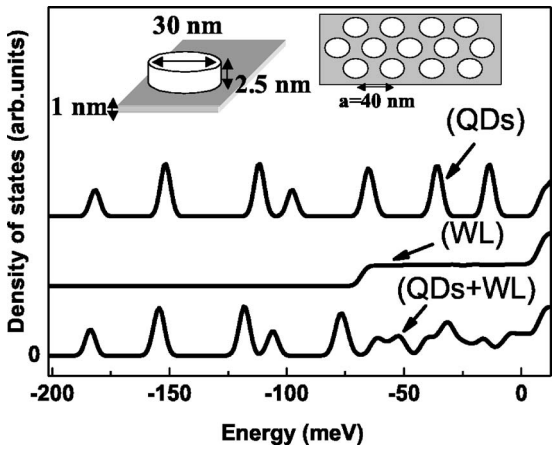

FIG. 1. Electronic density of states of a QD superlattice, a WL, and a QD superlattice on a WL ($C=51\%$). The difference between (QD)+(WL) and (QD+WL) systems is a coupling effect evidence. The figure inclusion represents the QD and WL with their dimensions.

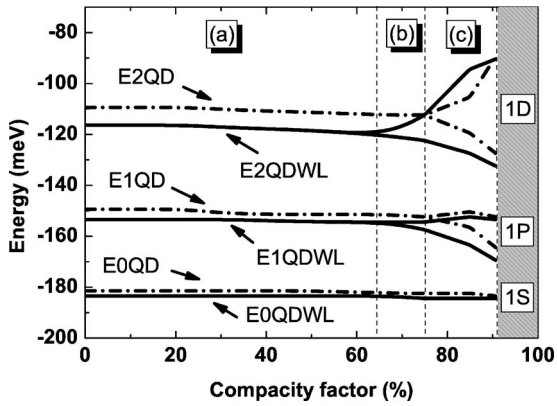

FIG. 2. A comparison between (QD+WL) and (QD) energies, for 1S, 1P, and 1D levels depending on the compacity factor. Effects of weak QD/WL coupling (a), WL-assisted inter-QDs weak coupling (b), WlaiQD coupling, and direct inter-QD strong coupling (c).

formed numerically, with a mixed basis of localized Wannier states $|\varphi_n(\vec{r})\rangle$ and plane waves $|\vec{k}\rangle$:[22,23]

$$|\Psi(\vec{r})\rangle = \sum_n c_n|\varphi_n(\vec{r})\rangle + \sum_{\vec{k}} c_{\vec{k}}|\vec{k}\rangle. \quad (2)$$

Localized Wannier states are Bessel-like functions allowing the continuity of the wave function between the QD and the barrier, taken from Ref. 26, Eq. (32).

The calculations are performed for the conduction band of InAs/InP (311)B QDs. These QDs can be considered as truncated cylindrical objects in a first approximation (Fig. 1). Their radius is $R=15$ nm and their height upside the WL is $L=2.5$ nm. The WL thickness Hw is equal to 1 nm,[10] so that the global confinement height in the z direction is 3.5 nm for QDs. The inclusion of localized Wannier states allows us to have a better calculation convergence, in describing the (WL+QD) system, in respect of our problem geometry. Calculations are performed for a 2D QD hexagonal lattice, where the QDs are located at the lattice nodes. C is the compacity factor (ratio between the surface covered by the QDs and the WL surface), $C=2\pi R^2/\sqrt{3}a^2$, where a is the lattice parameter.

The FT potential for the QD lattice is then

$$V_{\vec{k},\vec{k}'QD} = -V_0\frac{2\pi R^2 L}{\sqrt{3}a^2} j_1c(|\vec{G}_t - \vec{G}'_t|R/a) \times \mathrm{sinc}(|k_z - k'_z|L/2)e^{-ik_z[(L+Hw)/2]}, \quad (3)$$

with $j_1c(x)=J_1(2\pi x)/\pi x$, and $\mathrm{sinc}(x)=\sin(x)/x$ where J_1 is the first-order Bessel function, $\vec{G}_t$ is a vector of the reciprocal lattice in the (xy) plane, and k_z is the projection of the $\vec{k}$ vector along the z axis. The FT potential for the WL is

$$V_{\vec{k},\vec{k}'WL} = -V_0 Hw\ \mathrm{sinc}(|k_z - k'_z|Hw/2)\,\delta(\vec{G}_t - \vec{G}'_t). \quad (4)$$

Thus, the FT potential for the whole structure is

$$V_{\vec{k},\vec{k}'} = V_{\vec{k},\vec{k}'QD} + V_{\vec{k},\vec{k}'WL}. \quad (5)$$

III. RESULTS

A. Effect of coupling on QD density of states

Electronic densities of states for QDs alone (with $L=3.5$ nm), WL alone, and for the association of QDs and WL, (QDs+WL), are plotted in Fig. 1, for $a=40$ nm (i.e., $C=51\%$). A Gaussian shape with full width at half-maximum equal to 5 meV is assumed for inhomogeneous broadening. As shown in Fig. 1, the (QDs+WL) system density of states is different from sum of the separate QD (0D) and WL (2D) densities of states, in the $[-100;0]$ meV energy range. Energy spectrum modification is evidence of the QD/WL coupling effect. The 2D WL electronic density of states is fragmented with coupling. Therefore, the (QD+WL) system has to be considered as a unique system, and QDs and WL cannot be studied independently. In the $[-200;-100]$ meV energy range, the 0D QD electronic densities of states are similar for (QDs) and (QDs+WL); a small energy shift is the only consequence of the coupling effect.

This coupling effect is, in fact, strongly dependent on the QDD. The coupling between QDs is greatly enhanced for a large compacity factor (C), i.e., for a high QDD. In order to estimate the role of the WL on this coupling, we can plot the evolution of the QD energy levels with or without a WL, for various compacity factors. Figure 2 represents the 1S, 1P, and 1D energy levels in the QDs, and their evolution with C. For isolated QDs, 1P and 1D are degenerated states (because of cylindrical symmetry), and a splitting of these energy levels is associated with the coupling.

For a low QDD, i.e., a [0;64]% compacity range [Fig. 2, domain (a)], we note a difference in energy between the (QDs) and (QDs+WL) system.[16] This is due to the intrinsic difference of confinement in the structure.[24] In the presence of a WL, wave functions of isolated QDs can extend into the WL area, so that energies of these (QDs+WL) states are lower than corresponding (QD) energies. This effect is more important for higher-energy levels 1P and 1D, because of their high wave function spatial extension. In domain (a), the QD/WL coupling is clearly visible on high-energy states

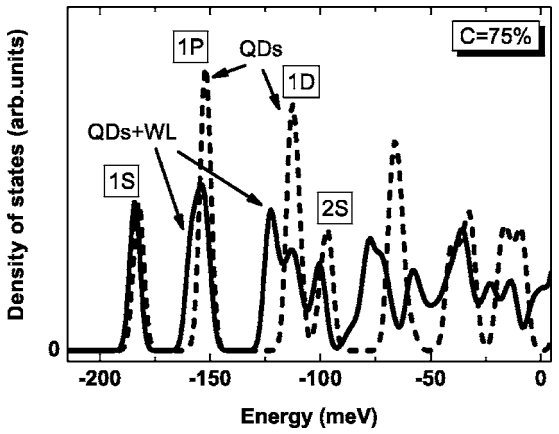

FIG. 3. (QD+WL) and (QD) densities of states for a sample with a 75% compacity factor. The figure highlights the WL influence on splitting and miniband effects.

(Fig. 1), but inter-QDs coupling is negligible (no splitting or miniband effects).

For $C=64\%$ to $C=75\%$ [Fig. 2, domain (b)] (i.e., for densities from 8.4×10^{10} to 1.0×10^{11} cm^{-2} that is around the highest experimental QD densities in this system[27]), we observe a clear difference between (QDs+WL) and (QDs). The P and D splitting effect, due to inter-QD coupling, occurs for (QDs+WL) while there is no splitting for (QDs). Figure 3 shows electronic densities of states for (QD+WL) and (QDs) with a 75% compacity factor (1.0×10^{11} cm^{-2}). The 1S state does not sensitively change with the addition of a WL. The 1P state, which is twice degenerated for isolated QDs, becomes lightly splitted in the presence of the WL. It is the first evidence of the WL role in the inter-QD coupling. The degenerated 1D state is strongly splitted in the presence of WL. In Fig. 3, the 2S density of states decreases with the presence of the WL. This is due to a miniband effect on these levels. This miniband effect is more visible on high-energy excited states. QD excited states lose their 0D character, and thus the classical artificial atom picture becomes inappropriate. It is the second evidence of the WL role in the inter-QD coupling. In Fig. 2, domain (b), WL enhances the weak inter-QD coupling. We call this phenomenon WL-assisted inter-QD coupling (WLaiQD).

For $C=75\%$ to $C=91\%$ [Fig. 2, domain (c)] (91% is the maximum compacity for an hexagonal 2D QD superlattice), a splitting occurs even for QDs alone. In this configuration, each dot is very close to its neighbors. These are strong coupling conditions. Then, in domain (c) we have both direct inter-QD coupling and WLaiQD. For $C=91\%$, the difference between (QD+WL) and (QD) corresponding energies becomes very small. Each dot is in contact with its neighbors. Direct inter-QD coupling is the dominant effect.

B. Effect of coupling on WL density of states

Up until now, it is clear that WL increases the lateral inter-QD coupling by modifying the QDs electronic density of states. We shall now consider the coupling influence on WL states. Figure 1 shows a WL density of states modification, in the $[-100,0]$ meV range. This effect can be correlated with experimental absorption spectra,[11] and TRPL spectra,[12,13] which show WL "excited optical transitions." We propose to describe the WL structuring as a consequence of the WL-assisted inter-QD coupling. QD and WL optical transitions are difficult to identify.[11] From a traditional uncoupled point of view, QD states have a purely 0D character, and WL states have a purely 2D character. From our calculation, we see that QD and WL ground and excited states are not clearly distinguishable on the calculated densities of states. Our hypothesis, based on calculation results, is to consider that these states have neither a 0D character, nor a 2D character, but a hybrid 2D/0D character. As a consequence, the electronic wave functions for the $[-75;0]$ meV energy range, should be localized partly in the QDs, and partly in the WL. An electronic wave function in real space is obtained using the FT of the eigenstates. Figure 4 shows one result for a 2D-hexagonal superlattice of cylindrical QDs. The electronic probability density for WL states are calculated for an uncoupled ($C=8\%$) and a coupled ($C=75\%$) configuration, and represented in the (x,y) plane (Fig. 4). This probability is calculated for the lowest-energy WL states in both configurations. White circles represent the positions of the cylindrical QDs in the (x,y) plane. White areas represent a maximum of probability density equal to 0.84 in an arbitrary scale. This state is mainly located in the WL for

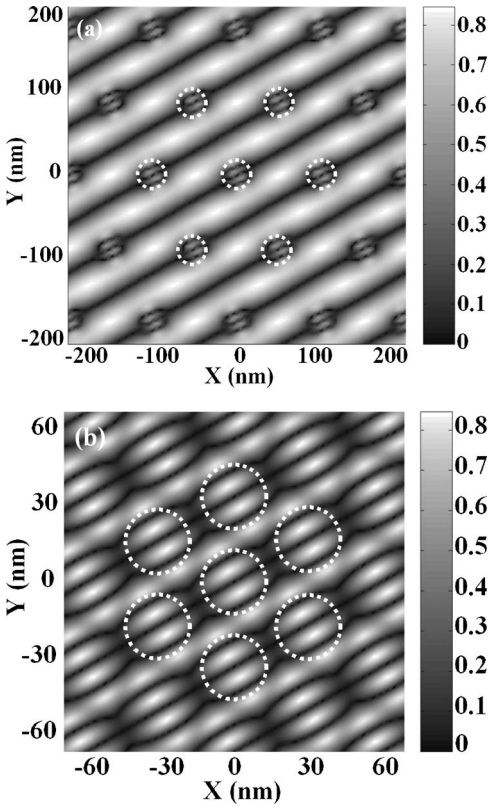

FIG. 4. Probability density of low-energy WL states: wave function spatial variations for a 2D-hexagonal superlattice of cylindrical QDs on a WL. A WL state is represented for an uncoupled (a) and a coupled (b) configuration. WL states lose their 2D character with coupling. Density is in arbitrary units, with a maximum at 0.84.

the uncoupled configuration. In the coupled configuration, we can clearly see that a large part of the WL wave function spreads into the QD region.[16–18] There is even a local maximum of probability density in the QD region. Moreover, the electronic wave function in the uncoupled configuration is infinitely delocalized along one axis. With strong coupling, this WL state seems to fill a particular localized space area, producing a "pseudo-0D confinement." This evidences that WL states have no longer a purely 2D character, but are rather hybrid 2D/0D states. These kinds of hybridization have been described previously for quantum wells.[28] The same analysis on the whole energy spectrum shows that QD fundamental and first excited states are still localized for a high QDD. On the other hand, lower-energy WL wave functions lose their 2D character, and higher-energy QD wave functions lose their 0D character. This explains why a WL contribution in the electronic density of states spectrum gets structured with increasing coupling.

IV. APPLICATION TO REAL QUANTUM DOTS

From a QD device point of view, this coupling effect can have a positive impact on carrier capture rates from the barrier into the QD region, and carrier redistribution between quantum dots, provided the ground state keeps an atomic-like density of state.[29] This effect is expected for a high QD density. Such a density can be obtained by growing InAs on quaternary alloy $In_{0.2}Ga_{0.8}As_{0.435}P_{0.565}$ on an InP (311)B substrate with an optimized flux of As_2.[30,31] Figure 5(a) shows an Atomic Force Microscopy (AFM) picture of these QDs. The QD density is 8.10^{10} cm^{-2} and the average radius of these QDs is 15 nm in this sample. In this range of densities, QDs become organized in the (x,y) plane.[31] Figure 5(b) is obtained by calculating the 2D-Fast Fourier Transformation (FFT) of Fig. 5(a). The presence of QD self-organization is pointed out by the observation of intensity spots on the 2D-FFT picture along the preferential axis. From theses observations, a 2D square lattice of InAs/InGaAsP QDs can be assumed for the electronic structure calculation. For such a structure, the confinement potential is equal to $V_0 = 391$ meV in all the confining volume. The compacity factor is given by $C = \pi R^2/a^2$ in this square lattice. Figure 6 shows the evolution of electronic energy levels 1S, 1P, 1D for a square lattice of InAs/InGaAsP QDs as a function of the compacity factor, with or without a WL. Coupling occurs for a lower compacity factor in the square lattice than in the hexagonal lattice. An arrow indicates that our QDs have a 59% compacity factor, which is the limit between domain (b) (WlaiQDs coupling) and domain (c) (direct inter-QD coupling). From this calculation, a miniband effect due to the WL is expected in the QD electronic structure of such a sample, even if it is not the highest density that can be reached in this system. Further experimental investigations are on the way to try to evidence this phenomenon.

V. CONCLUSION

The electronic WlaiQD coupling and its consequences were studied in this work. We used a FT-Schrödinger equation on a mixed basis of plane waves and localized states. We showed that (QD+WL) system has to be considered a unique and coupled system. We found clear evidence of QD/WL coupling, WL-assisted inter-QD coupling, and direct inter-QD coupling influence on QD electronic properties. Splitting and miniband effects appear that highlights the

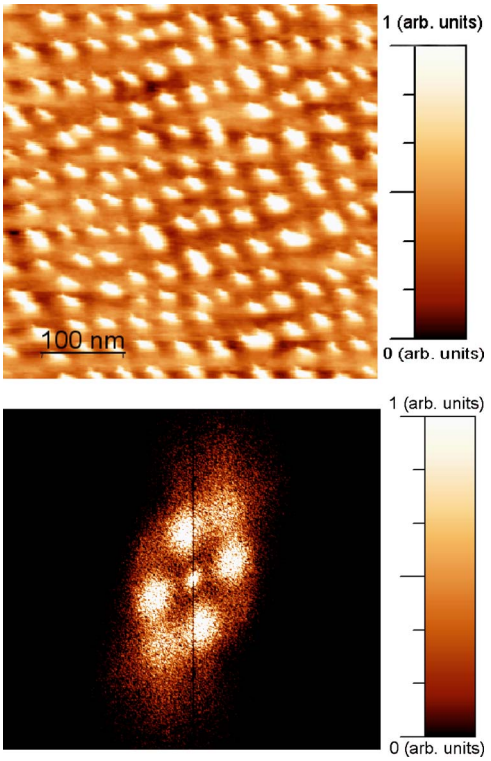

FIG. 5. (Color online) Atomic force microscopy picture of InAs/InGaAsP QDs with optimized As_2 flux on a (0.5×0.5) μm^2 InP (311)B surface (a) reveals a high density and a squarelike lattice organization of the QDs. Strong and localized spots along a particular axis on the 2D-Fast Fourier Transformation (b) of this picture is a evidence of QD self-organization.

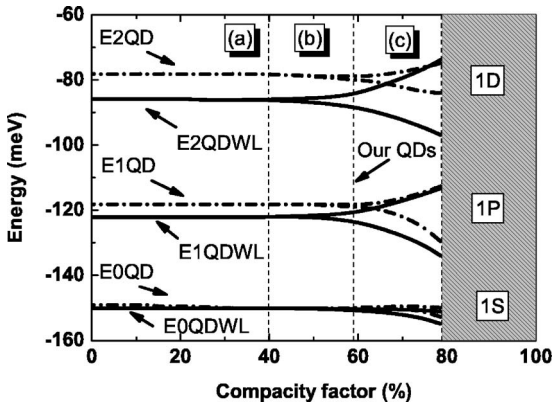

FIG. 6. A comparison between (QD+WL) and (QD) energies, for 1S, 1P, and 1D levels depending on the compacity factor for InAs/InGaAsP QDs on a square lattice. Effects of weak QD/WL coupling (a), WL-assisted inter-QD weak coupling (b), WlaiQD coupling and direct inter-QDs strong coupling (c). Calculations predict a WlaiQD coupling for the sample of Fig. 5.

limitation of the artificial atom picture. We demonstrated that the WL should no longer be considered a pure 2D-like confining object, but rather a hybrid 2D/0D object. Finally, an application to a real QD sample has been performed. This simple model is suitable to describe the coupling effect. From now, we can qualitatively understand the WL structuring on absorption[11] and TRPL spectra[12,13] as a direct consequence of WLaiQD coupling. This model has to be extended to heavy hole and light hole states, to inhomogeneous QD distributions and to absorption calculations. New experiments on samples with different QDD, and new absorption calculations are needed in order to compare the calculation and experiment in a quantitative way. This analysis should also be considered for ultrafast QD-based optoelectronic devices.[16,29] The hybrid 2D/0D character for WL lower-energy states, and QD higher-energy states, could change carrier capture rates from the barrier into the QD region, whereas the QD ground state keeps an atomiclike character. It is also expected to have an impact on the charge redistribution process.[29]

*Electronic address: charles.cornet@ens.insa-rennes.fr

[1] M. Grundmann, D. Bimberg and N. N. Ledentsov, *Quantum Dot Heterostructures* (Wiley, Chichester, 1998).

[2] L. Banyai and S. W. Koch, *Semiconductor Quantum Dots, World Scientific Series on Atomic, Molecular and Optical Physics* (World Scientific, Singapore, 1993), Vol. 2.

[3] M. Sugawara, *Self-Assembled InGaAs/GaAs Quantum Dots, Semiconductors and Semimetals* (Academic, Toronto, 1999), Vol. 60.

[4] Zh. I. Alferov, *Quantum Wires and Dots Show the Way Forward* (III-Vs Rev., City, 1998), Vol.11, p. 47.

[5] G. T. Liu, A. Stintz, H. Li, T. C. Newell, A. L. Gray, P. M. Varangis, K. J. Malloy, and L. F. Lester, IEEE J. Quantum Electron. **36**, 1272 (2000).

[6] H. Saito, K. Nishi, A. Kamei, and S. Sugou, IEEE Photonics Technol. Lett. **12**, 1298 (2000).

[7] O. B. Shcheckin and D. G. Deppe, IEEE Photonics Technol. Lett. **14**, 1231 (2002).

[8] S. Frechengues, N. Bertru, V. Drouot, B. Lambert, S. Robinet, S. Loualiche, D. Lacombe and A. Ponchet, Appl. Phys. Lett. **74**, 3356 (1999).

[9] C. Paranthoën, N. Bertru, B. Lambert, O. Dehaese, A. Le Corre, J. Even, S. Loualiche, F. Lissillour, G. Moreau and J. C. Simon, Semicond. Sci. Technol. **17**, L5 (2002).

[10] C. Paranthoën, C. Platz, G. Moreau, N. Bertru, O. Dehaese, A. Le Corre, P. Miska, J. Even, H. Folliot, C. Labbé, G. Patriarche, J. C. Simon, and S. Loualiche, J. Cryst. Growth **251**, 230 (2003).

[11] C. Cornet, C. Labbé, H. Folliot, N. Bertru, O. Dehaese, J. Even, A. Le Corre, C. Paranthoen, C. Platz, and S. Loualiche, Appl. Phys. Lett. **85**, 5685 (2004).

[12] P. Miska, C. Paranthoen, J. Even, O. Dehaese, H. Folliot, N. Bertru, S. Loualiche, M. Senes, and X. Marie, Semicond. Sci. Technol. **17**, L63 (2002).

[13] P. Miska, J. Even, C. Paranthoen, O. Dehaese, H. Folliot, S. Loualiche, M. Senes, and X. Marie, Physica E (Amsterdam) **17**, 56 (2003).

[14] P. Miska, C. Paranthoen, J. Even, N. Bertru, A. Le Corre, and O. Dehaese, J. Phys.: Condens. Matter **14**, 12301 (2002).

[15] C. Kammerer, G. Cassabois, C. Voisin, C. Delalande, Ph. Roussignol, and J. M. Gérard, Phys. Rev. Lett. **87**, 207401 (2001); C. Kammerer, G. Cassabois, C. Voisin, C. Delalande, Ph. Roussignol, A. Lemaître, and J. M. Gérard, Phys. Rev. B **65**, 033313 (2002); C. Kammerer, C. Voisin, G. Cassabois, C. Delalande, Ph. Roussignol, F. Klopf, J. P. Reithmaier, A. Forchel, and J. M. Gérard, *ibid.* **66**, 041306(R) (2002); C. Kammerer, G. Cassabois, C. Voisin, M. Perrin, C. Delalande, Ph. Roussignol, and J. M. Gérard, Appl. Phys. Lett. **81**, 2737 (2002).

[16] R. V. N. Melnik and M. Willatzen, in *Proceedings of the 2002 International Conference on Modeling and Simulation of Microsystems*, Nano Science and Technology Institute, 2002, pp. 506–509.

[17] H. T. Johnson, R. Bose, H. D. Robinson, and B. B. Goldberg, Appl. Phys. Lett. **82**, 3382 (2003).

[18] H. T. Johnson, V. Nguyen, and A. F. Bower, J. Appl. Phys. **92**, 4653 (2002).

[19] H. D. Robinson and B. B. Goldberg, Physica E (Amsterdam) **6**, 444 (2000).

[20] H. D. Robinson, B. B. Goldberg and J. L. Merz, Phys. Rev. B **64**, 075308 (2001).

[21] H. D. Robinson, B. B. Goldberg, and J. L. Merz, in *Proceedings of the Materials Research Society, 1999*, Vol. 571, p. 189.

[22] G. W. Bryant, Phys. Rev. B **40**, 1620 (1989).

[23] N. V. Tkach, A. M. Makhanets, and G. G. Zegrya, Semicond. Sci. Technol. **15**, 395 (2000).

[24] S. Lee, O. L. Lazarenkova, P. von Allmen, F. Oyafuso, and G. Klimeck, Phys. Rev. B **70**, 125307 (2004).

[25] P. Miska, J. Even, C. Platz, B. Salem, T. Benyattou, C. Bru-Chevalier, G. Guillot, G. Bremond, Kh. Moumanis, F. H. Julien, O. Marty, C. Monat, and M. Gendry, J. Appl. Phys. **95**, 1074 (2004).

[26] S. Le Goff and B. Stébé, Phys. Rev. B **47**, 1383 (1993).

[27] J. W. Jang, S. H. Pyun, S. H. Lee, I. C. Lee, W. G. Jeong, R. Stevenson, P. D. Dapkus, N. J. Kim, M. S. Hwang, and D. Lee, Appl. Phys. Lett. **85**, 3675 (2004).

[28] C. Metzner, M. Hofmann, and G. H. Döhler, Phys. Rev. B **58**, 7188 (1998).

[29] Y. Ducommun, M. Kroutvar, M. Reimer, M. Bichier, D. Schuh, G. Abstreiter, and J. J. Finley, Appl. Phys. Lett. **85**, 2592 (2004).

[30] P. Caroff, N. Bertru, C. Platz, O. Dehaese, A. Le Corre, and S. Loualiche, J. Cryst. Growth **273**, 357 (2005).

[31] P. Caroff, N. Bertru, A. Le Corre, O. Dehaese, T. Rohel, H. Folliot, and S. Loualiche (unpublished).